Journal of Power Sources 206 (2012) 103–107

Contents lists available at SciVerse ScienceDirect

Journal of Power Sources

journal homepage: www.elsevier.com/locate/jpowsour

Short communication

Effect of Se in Co-based selenides towards oxygen reduction electrocatalytic activity

Dongjiang Zhao[a,b], Sheng Zhang[a], Geping Yin[a,*], Chunyu Du[a], Zhenobo Wang[a], Jie Wei[a]

[a] State Key Laboratory of Urban Water Resource and Environment, School of Chemical Engineering and Technology, Harbin Institute of Technology, Harbin 150001, China
[b] Department of Chemical and Medical Engineering, Suihua University, Suihua 152061, China

ARTICLE INFO

Article history:
Received 10 October 2011
Received in revised form
25 November 2011
Accepted 1 January 2012
Available online 20 January 2012

Keywords:
Oxygen reduction
Non-noble metal catalyst
Cobalt selenide
Polymer electrolyte membrane fuel cells

ABSTRACT

In this study, Co-based selenides with various selenium contents have been synthesized by heating dodecacarbonyltetracobalt [$Co_4(CO)_{12}$] and elemental selenium in 1,6-hexanediol solvent under refluxing conditions. The synthesized catalyst powders are characterized by X-ray diffraction (XRD) and scanning electron microscopy (SEM). The samples exhibit cauliflower-like surface morphologies and reveal the crystalline characteristics of orthorhombic $CoSe_2$ compound. Electrocatalytic performances of the Co–Se compounds for the oxygen reduction reaction in 0.5 M H_2SO_4 electrolyte are evaluated by rotating disk electrode (RDE). Co–Se catalysts are electrochemical stable in the potential range of 0.05–0.80 V (vs. NHE). The catalytic activity changes with increasing selenium content, and the highest activity is obtained at 67.1 mol% Se in the catalyst, which can be attributed to the modification of selenium element on the electronic structure of cobalt.

1. Introduction

Polymer electrolyte membrane fuel cells (PEMFCs) are regarded as one of the most promising power sources for transportation, generation of power, and portable electronic devices, etc., due to their high energy-conversion efficiency, low temperature of operation, and zero or low emission [1–5]. At present, the most commonly used catalysts for oxygen reduction reaction (ORR) in PEMFCs are platinum and its alloys with other metals, a precious and scarce metal [3,6]. For resource and economic reasons, partial or complete replacement of platinum metal catalysis has attracted great attention [7,8]. Many non-platinum catalysts for the ORR have been synthesized and investigated in acid medium, and have shown promising activities such as transition metal chalcogenides [9–11], macrocycles containing iron or cobalt metal [12–14], transition metal nitrides [15–17] and transition metal alloys [18,19].

Among the non-platinum catalysts reported, the ruthenium-based chalcogenide catalysts have high catalytic activity and stability towards the ORR in H_2SO_4 electrolyte solution. However, the use of ruthenium does not avoid the cost and resource issue. Therefore, it is significant to explore non-precious transition metal chalcogenide catalysts. Recently, Co–Se [20–22], FeS_2 [23] and CoS_2 [24] based thin films prepared by magnetron sputtering have displayed appreciable catalytic activity towards the ORR in acidic medium. Vayner et al. [25] reported that the catalytic activity of the heat-treated Co–Se catalyst for the ORR was remarkably increased, compared to the as-refluxed Co–Se catalyst. More recently, the $CoSe_2$/C nanoparticles synthesized by Feng et al. [26–28] display promise as non-noble metal electrocatalysts for the ORR with an open circuitry potential (OCP) of 0.81 V (NHE) in 0.5 M H_2SO_4, and have higher methanol tolerance as compared to Pt/C catalyst. The crystalline $CoSe_2$ with the pyrite structure prepared by Zhu et al. [29] has superior performance for the ORR compared with the Co–Se thin films. Fe_3O_4 nanoparticles decorated $CoSe_2$–DETA (DETA stands for diethylenetriamine) hybrid nanobelts (NBs) present better ORR activity than original $CoSe_2$–DETA NBs, due to synergetic effect between Fe_3O_4 and $CoSe_2$ [30]. However, the dependence of the ORR catalytic activity on selenium content in the cobalt selenides has not been reported.

In the present work, the influences of selenium content on catalytic activity of the Co–Se catalysts for the ORR in acidic medium were investigated. The cobalt selenides with various selenium content were synthesized by reacting dodecacarbonyltetracobalt [$Co_4(CO)_{12}$] and selenium in 1,6-hexanediol solvent under refluxing condition. The Co–Se catalysts exhibit high electrochemical stability in the potential range of 0.05–0.80 V (vs. NHE). The catalytic activity towards the ORR changes with selenium content

* Corresponding author at: School of Chemical Engineering and Technology, Harbin Institute of Technology, No. 92, West Da-Zhi Street, Harbin 150001 China. Tel.: +86 451 86413707; fax: +86 451 86413707.
E-mail address: yingeping@hit.edu.cn (G. Yin).

0378-7753/$ – see front matter © 2012 Elsevier B.V. All rights reserved.
doi:10.1016/j.jpowsour.2012.01.018

in the catalysts, and the highest value is reached at 67.1 mol% Se with the OCP value of 0.79 V (vs. NHE). The relationship between the electronic structures modified by selenium and the corresponding catalytic activity for the cobalt–selenium compounds was explored.

2. Experimental

2.1. Catalyst preparation

The Co–Se catalysts were synthesized by reacting dodecacarbonyltetracobalt [$Co_4(CO)_{12}$] (Alfa Aesar) and elemental selenium (Alfa Aesar) in a chemical reactor containing 150 mL of 1,6-hexanediol (Alfa Aesar) solvent under refluxing conditions for 5 h, when Se molar ratio in the catalysts was chosen at 33.3, 50.0, 60.0, 66.7 and 71.4 mol%. Then, the system was cooled to room temperature and the precipitated powders were recovered from the reaction medium with ethyl acetate and ultra-pure water. The powders were ultrasonically washed with ethyl ether, to eliminate the un-reacted precursor and the organic reaction medium. The powders were dried overnight at room temperature.

2.2. Physical characterization

The surface morphology of the powders was imaged using a scanning electronic microscope (SEM, FEI Quanta 200), with a 15 kV electron beam. Elemental analysis was performed by an energy dispersive X-ray spectroscopy (EDS) coupled with the SEM. The structural analysis of the compounds was performed by X-ray diffractometer (XRD, Rigaku Corporation D/max-rB) operated at 40 mA and 45 kV using a monochromatic Cu Kα radiation. The XRD patterns were recorded between 20° and 80° at a scanning rate of 5° per minute. The diffractograms measured were identified using the JCPDS standard cards.

2.3. Electrochemical measurements

The glassy carbon disk with a cross-sectional area of 0.1256 cm^2 was employed as the working electrode for the rotating disk electrode (RDE) studies. Ink-type working electrodes were prepared as follows: 4 mg of the catalyst was added to 1 mL ultra-pure water, and the resulting mixture was sonicated for 5 min. 8 μL of an ink containing 0.25 mg cm^{-2} of the catalyst was deposited onto the glassy carbon surface. After drying, 6.5 μL of a mixture of Nafion solution (5 wt%, Du Pont, 1100 EW) and ethanol was coated onto the catalyst layer surface and dried at room temperature [31].

The electrochemical experiments were completed in a single three-electrode test cell at 25 °C. Platinum wire and Hg/Hg_2SO_4/0.5 M H_2SO_4 electrode was used as the counter and reference electrode, respectively. The RDE electrochemical measurements were performed on an electrochemical workstation (Model CHI 660 C) and a rotation speed controller (Model ATA-1 B). The potential values reported in this paper refer to the normal hydrogen electrode (NHE). A 0.5 M H_2SO_4 electrolyte solution was prepared from ultra-pure water. Prior to all electrochemical measurements, the Co–Se electrodes were activated by scanning potential (cyclic voltammetry) between 0.05 V and 0.80 V (NHE) at 25 mV s^{-1} for 20 min in 0.5 M H_2SO_4 solution outgassed with purified nitrogen. Then, the solution was saturated with oxygen for 30 min and maintained this oxygen atmosphere above the solution surface during the current–potential measurements. The catalytic activities and kinetic properties of the Co–Se catalysts for the ORR were investigated by using RDE measurements from the open circuit potential (OCP) to 0.05 V (vs. NHE) at a 10 mV s^{-1} rate. The rotation rates ranged from 100 to 2500 rpm.

3. Results and discussion

3.1. Material characteristics

The measured average Se molar ratio in the synthesized Co–Se compounds is 31.7, 49.6, 61.2, 67.1 and 70.9 mol% as deduced from EDS data from the atomic percent chemical analysis, indicating that the designed and measured composition is basically consistent. Fig. 1 shows SEM images of the as-synthesized Co–Se powders contained 31.7 mol% Se (a), 67.1 mol% Se (b) and 70.9 mol% Se (c). It can be observed that all samples are aggregates and exhibit cauliflower-like surface morphologies. The characteristics of the cauliflower-like images have no obvious differences with the increase of Se content in the Co–Se compounds.

The XRD spectra of the as-synthesized Co–Se catalysts contained 31.7 mol% Se (a), 67.1 mol% Se (b) and 70.9 mol% Se (c) are shown in Fig. 2. Obviously, the powders contain different phase structures. The similarity in positions for the diffraction peaks near $2\theta = 30.5°$, 34.4° and 36.0° measured from the Co–Se powders, indicates that all the powders contain similar structures. Comparison with the JCPDS database (PDF 10-0408) indicates that the crystalline phase reveals the crystalline characteristics of orthorhombic $CoSe_2$ compound. Moreover, the un-reacted Se phase (relative to JCPDS-PDF 27-0601) is also found. The (1 1 1) crystal plane near $2\theta = 34.4°$ has the highest intensity among the diffraction peaks of the orthorhombic $CoSe_2$, and the intensity changes significantly with rising selenium content in the Co–Se catalysts, and the maximal intensity is obtained for 67.1 mol% Se. This result indicates that the Co–Se powder contained 67.1 mol% Se displays the highest degree of crystallinity.

3.2. Electrochemical characterization

3.2.1. Cyclic voltammetric characterization

Fig. 3 shows the cyclic voltammograms for the Co–Se catalyst contained 31.7 mol% Se (a), 67.1 mol% Se (b) and 70.9 mol% Se (c) in 0.5 M H_2SO_4 solutions under nitrogen atmosphere. The cyclic voltammograms of the three Co–Se catalysts reach a steady state after eleven, six, five scan cycles in the potential range of 0.05–0.80 V (vs. NHE), respectively. Generally, cobalt is thermodynamically unstable due to electrochemical oxidation [32]. However, no anodic oxidation currents could be observed in the cyclic voltammograms, indicating that the Co-based chalcogenides are electrochemical stable. This may be attributed to modification of selenium on the electronic structure of metal cobalt, because selenium element can play a role in preventing the electrochemical oxidation of metals in transition metal chalcogenides [33].

Cyclic voltammograms of the Co–Se catalysts with various selenium contents were measured in O_2-saturated 0.5 M H_2SO_4 solution, while the potential is swept between 0.08 and 0.90 V (vs. NHE), as shown in Fig. 4. It can be observed that the peak potentials and peak current densities for the ORR are affected by Se contents in the Co–Se catalysts. The highest peak potential (0.42 V, vs. NHE) and largest peak current density (0.31 mA cm^{-2}) indicate that the Co–Se catalyst contained 67.1 mol% Se has the best electrocatalytic activity towards the ORR. Since the elemental selenium [22] and metal cobalt [34,35] do not present catalytic activity for the ORR, the activity of the Co–Se catalysts should be the result of interaction between cobalt and selenium element.

3.2.2. Oxygen reduction in RDE measurements

In order to study the influences of Se content on catalytic performances of the Co–Se catalysts, the current–potential curves of the catalysts with various selenium contents for the ORR were measured by RDE with rotation rate of 1600 rpm and sweep rate of 10 mV s^{-1} in O_2-saturated 0.5 M H_2SO_4 at 25 °C (inset on the top

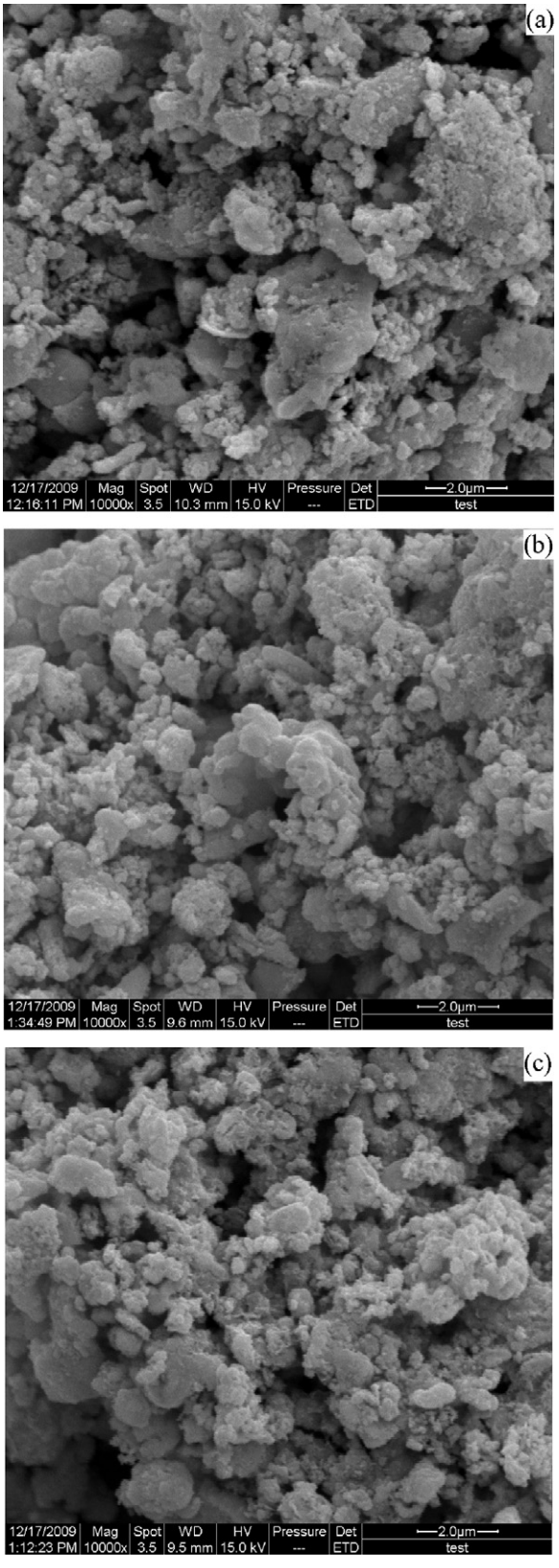

Fig. 1. SEM micrographs of the as-synthesized Co–Se catalyst powders: (a) 31.7 mol% Se, (b) 67.1 mol% Se, and (c) 70.9 mol% Se.

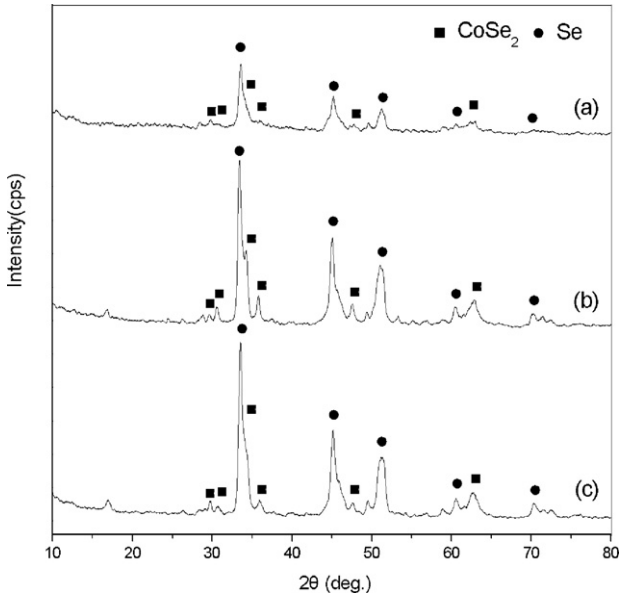

Fig. 2. XRD patterns for the Co–Se catalyst powders. (a) 31.7 mol% Se, (b) 67.1 mol% Se, and (c) 70.9 mol% Se.

in Fig. 4). It was observed that Se content obviously affects the catalytic activity in terms of current density. The current density of the Co–Se catalysts towards the ORR increases with rising selenium content until a maximum value at 67.1 mol% Se is reached. And then the enhancing selenium content would lead to a decrease in the current density. The result could be attributed to the highest degree of crystallinity for the Co–Se powder contained 67.1 mol% Se. The OCPs of the Co–Se catalysts with various selenium contents were measured, shown in Table 1. The OCP value of 0.79 V for the Co–Se catalyst contained 67.1 mol% Se is higher than that of $Co_{1-x}Se$ thin film (0.74 V), $Co_{1-x}Se$/C powder (0.78 V) [22] and $CoSe_2$/C obtained by in situ synthesis methods (0.72 V) [26]. The value is slightly lower than that of the $CoSe_2$/C (0.81 V) with orthorhombic [27] and pyrite structure [29].

The overall measured disk current density, j, is related to the diffusion-limited current density, j_d, and the kinetic current density, j_k, by the Koutecky–Levich equation [36]:

$$\frac{1}{j} = \frac{1}{j_k} + \frac{1}{j_d} = \frac{1}{j_k} + \frac{1}{B\omega^{1/2}} \quad (1)$$

where ω is the rotation rate in revolutions per minute, B is the Levich slope, given by:

$$B = 0.2nFC_O D_O^{2/3} \nu^{-1/6} \quad (2)$$

where D_O is the diffusion coefficient of oxygen, C_O is the oxygen solubility and ν is the kinematic viscosity, n is the number of electron transferred per molecule of O_2 reduced, and F is the Faraday constant.

Fig. 5 shows the Koutecky–Levich plots and the ORR curves (Inset on the top) collected on the RDE in O_2-saturated 0.5 M H_2SO_4 at 25 °C for the Co–Se catalyst contained 67.1 mol% Se. The ORR curves (Fig. 5 (inset)) indicate that a charge transfer kinetic control is observed above 0.65 V (vs. NHE), because the current density does not depend on rotation rate of the RDE in the potential

Table 1
Electrochemical property of the Co–Se catalysts with various Se content towards ORR in 0.5 M H_2SO_4.

Se content (mol%)	31.7	49.6	61.2	67.1	70.9
OCP (V, NHE)	0.75	0.78	0.79	0.79	0.79
n	1.9	2.7	3.1	3.3	3.4
$-b$ (V dec^{-1})	0.133	0.131	0.126	0.120	0.122
α	0.44	0.45	0.47	0.49	0.49
$j_0 \times 10^6$ (mA cm^{-2})	1.32	1.79	1.95	1.58	1.97

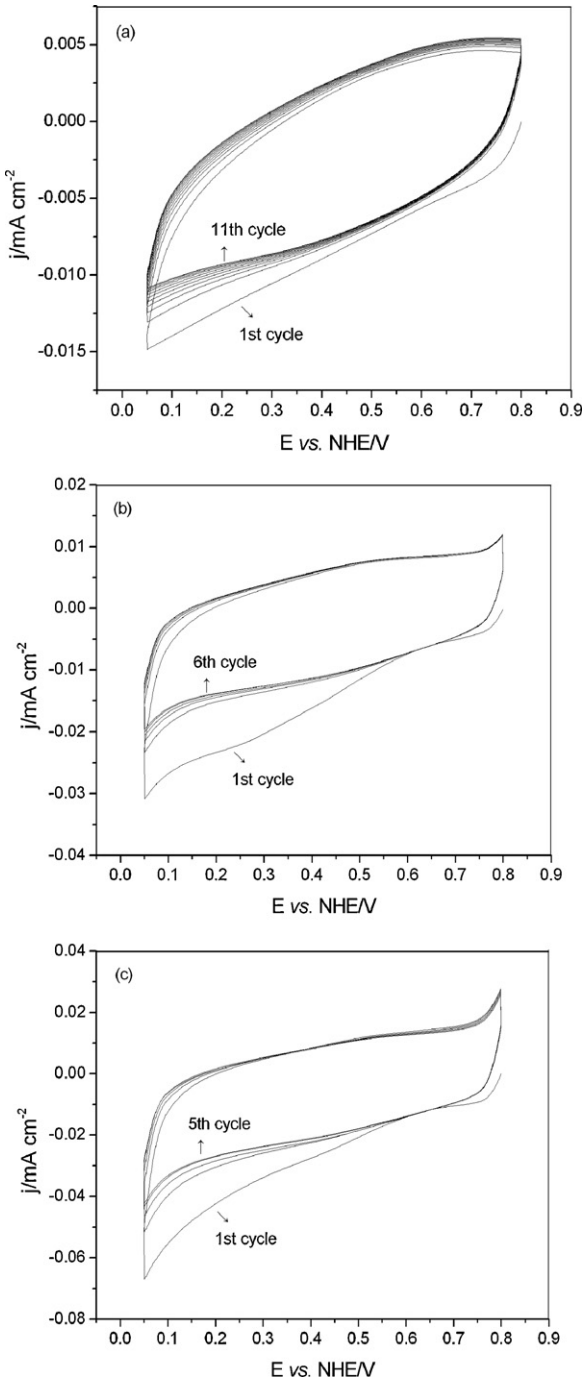

Fig. 3. Cyclic voltammograms of the Co–Se catalyst contained 31.7 mol% Se (a), 67.1 mol% Se (b) and 70.9 mol% Se (c) in 0.5 M H_2SO_4 purged with nitrogen at 25 °C. Scan rate is 25 mV s^{-1}.

range. The ORR is controlled by mixed kinetic-diffusion process at more cathodic potential than 0.65 V (vs. NHE). As the rotation rate increases, the diffusion currents are enhanced due to the increase of the oxygen diffusion through the RDE surface. The dependency relationship of the diffusion currents on the RDE rotating rate shows that the ORR kinetic processes on the Co–Se catalyst are controlled by the mass transport.

The plot of $1/j$ vs. $\omega^{-1/2}$ for potential range of 0.20–0.35 V (vs. NHE) yields a series of essentially parallel straight lines, having a slope value of B. The experimental average value of B is 7.70×10^{-2} mA cm^{-2} $rpm^{-1/2}$, while the theoretical value

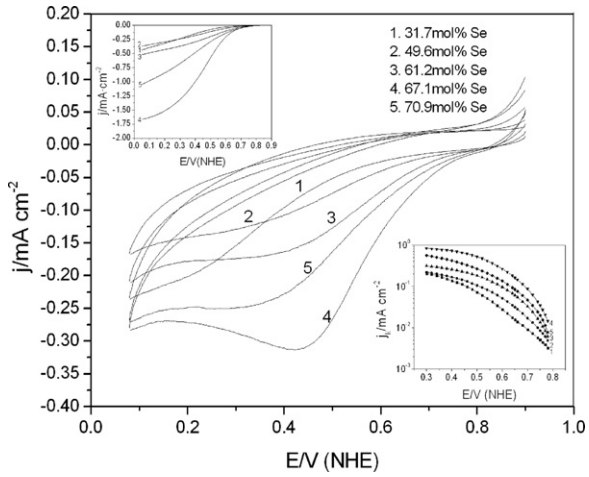

Fig. 4. Cyclic voltammograms and linear potential scan curves (Inset on the top) and mass transfer corrected Tafel plots (Inset on the bottom) for the Co–Se catalysts with various selenium contents in O_2-saturated 0.5 M H_2SO_4 at 25 °C. The scan rate of cyclic and linear sweep voltammetry is 25 mV s^{-1} and 10 mV s^{-1}, respectively. The rotation speed is 1600 rpm.

calculated for the four-electrons transfer in the ORR is 9.41×10^{-2} mA cm^{-2} $rpm^{-1/2}$. The theoretical value was calculated by using following data [37]: $D_O = 1.4 \times 10^{-5}$ cm^2 s^{-1}, $C_O = 1.1 \times 10^{-6}$ mol cm^{-3}, $\nu = 0.01$ cm^{-2} s and $n = 4e^-$. The linearity and parallelism of the all lines in Fig. 5 indicates that the electron number transferred per oxygen molecule and the active surface area of the catalyst does not obviously change in the potential range measured [38]. The B values of the other Co–Se catalysts were measured by the same method. The numbers of electrons transferred (n) during an oxygen molecule reduction on the Co–Se catalysts can be obtained by the B values, shown in Table 1. It is obvious that the numbers increase from 1.9 to 3.4 with rising selenium content in the Co-based chalcogenides. A value of $n = 3.3$ for the Co–Se catalyst contained 67.1 mol% Se was slightly lower than that of $CoSe_2$/C catalyst (3.5) [27]. And the ORR on the Co–Se catalysts is being performed via the mixed 2 and 4 electron processes.

The mass transfer corrected Tafel plots for the Co–Se catalysts were measured in oxygen saturated 0.5 M H_2SO_4 solution at 25 °C (Inset on the bottom in Fig. 4). The kinetic currents j_k, in the mixed

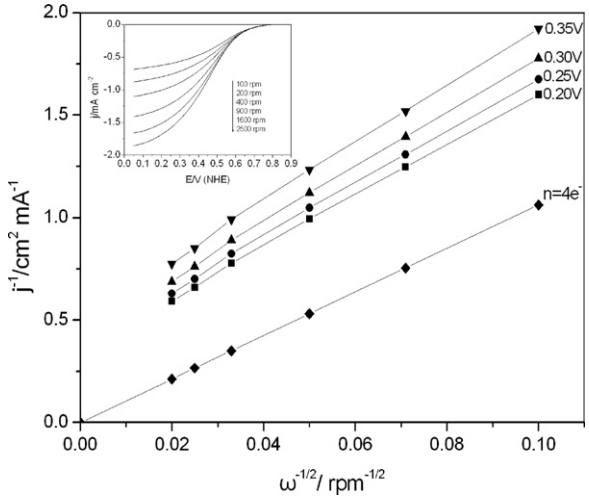

Fig. 5. Koutecky–Levich plots and ORR curves (Inset on the top) collected on the RDE in O_2-saturated 0.5 M H_2SO_4 at 25 °C for the Co–Se catalyst contained 67.1 mol% Se. The scan rate is 10 mV s^{-1}.

kinetic-diffusion region, were calculated by the following equation [39]:

$$j_k = j\frac{j_d}{j_d - j} \quad (3)$$

where $j_d/(j_d - j)$ is the mass transfer corrected function. The kinetic current density of the Co–Se catalysts towards the ORR changes with selenium content, the highest value is reached at 67.1 mol% Se. The Tafel slopes (b), exchange current densities (j_0) and transfer coefficient (α) of the catalysts are obtained in the potential range of 0.65–0.76 V (vs. NHE), are summarized in Table 1. The Tafel slope of $-120\,mV\,dec^{-1}$ for the Co–Se catalyst contained 67.1 mol% Se is comparable to results reported in the literature from Co–Se electrocatalysts. Examples of the results is $-133\,mV\,dec^{-1}$ for Co–Se thin film [22], $-125\,mV\,dec^{-1}$ for $CoSe_2$/C nanoparticles [26] and $-113\,mV\,dec^{-1}$ for $CoSe_2$ with the pyrite structure [29]. The density of state at Fermi level for cobalt could be changed by some electrons transfer from cobalt to selenium, and the density of state would play an important role in the chemical adsorption process of oxygen [40,41]. Therefore, the catalytic activity of the Co–Se compounds for the ORR might attribute to the electronic structure modified by selenium.

4. Conclusions

Cobalt selenides with various selenium content were synthesized in 1,6-hexanediol solvent under refluxing conditions, and exhibited high electrochemical stability in the potential range of 0.05–0.80 V (vs. NHE). The Co–Se catalysts had the crystalline characteristics of orthorhombic $CoSe_2$ compound and present cauliflower-like surface morphologies. And the catalytic activity of the Co–Se catalysts changes with selenium content, and the catalyst contained 67.1 mol% Se shows the highest activity towards oxygen reduction reaction in 0.5 M H_2SO_4 solution with the OCP value of 0.79 V (NHE). A Tafel slope of $-120\,mV\,dec^{-1}$ and a transfer coefficient of 0.49 for the Co–Se catalyst contained 67.1 mol% Se were obtained in the kinetic control region. The modification of selenium on the electronic structure of metal cobalt might be crucial factor to influence the catalytic performances of the Co–Se chalcogenide catalysts.

Acknowledgments

This work is financially supported by National Natural Science Foundation of China (Grant Nos. 50872027, 21106024, and 21173062), Ministry of Science and Technology of China (863 Program Grant No. 2009AA05Z111), Natural Scientific Research Innovation Foundation in Harbin Institute of Technology (XWQQ5750012411), and Fundamental Research Funds for the Central Universities (HIT.ICRST.2010006).

References

[1] J.D. Morse, Int. J. Energy Res. 31 (2007) 567–602.
[2] S. Zhang, Y.Y. Shao, G.P. Yin, Y.H. Lin, Angew. Chem. Int. Ed. 49 (2010) 2211–2214.
[3] J.J. Wang, G.P. Yin, H. Liu, R.Y. Li, R.L. Flemming, X.L. Sun, J. Power Sources 194 (2009) 668–673.
[4] Y.Y. Shao, S. Zhang, C.M. Wang, Z.M. Nie, J. Liu, Y. Wang, Y. Lin, J. Power Sources 195 (2010) 4600–4605.
[5] W.L. Xu, X.C. Zhou, C.P. Liu, W. Xing, T.H. Lu, Electrochem. Commun. 9 (2007) 1002–1006.
[6] S. Zhang, Y.Y. Shao, X.H. Li, Z.M. Nie, Y. Wang, J. Liu, G. Yin, Y. Lin, J. Power Sources 195 (2010) 457–460.
[7] Z. Chen, D. Higgins, A. Yu, L. Zhang, J. Zhang, Energy Environ. Sci. 4 (2011) 3167–3192.
[8] S. Zhang, Y.Y. Shao, G.P. Yin, Y.H. Lin, J. Power Sources 195 (2010) 1103–1106.
[9] O. Solorza-Feria, K. Ellmer, M. Gierstig, N. Alonso-Vante, Electrochim. Acta 39 (1994) 1647–1653.
[10] H. Cheng, W. Yuan, K. Scott, J. Power Sources 183 (2008) 678–681.
[11] A.S. Gago, D. Morales-Acosta, L.G. Arriaga, N. Alonso-Vante, J. Power Sources 196 (2011) 1324–1328.
[12] R.Z. Jiang, D. Chu, J. Electrochem. Soc. 147 (2000) 4605–4609.
[13] M. Lefevre, J.P. Dodelet, P. Bertrand, J. Phys. Chem. B 109 (2005) 16718–16724.
[14] H. Zhang, X. Yuan, L. Sun, X. Zeng, Q. Jiang, Z. Shao, Z. Ma, Int. J. Hydrogen Energy 35 (2010) 2900–2903.
[15] H. Zhong, H. Zhang, G. Liu, Y. Liang, J. Hu, B. Yi, Electrochem. Commun. 8 (2006) 707–712.
[16] L. Liu, J.W. Lee, B.N. Popov, J. Power Sources 162 (2006) 1099–1103.
[17] J. Tian, L. Birry, F. Jaouen, J.P. Dodelet, Electrochim. Acta 56 (2011) 3276–3285.
[18] W.E. Mustain, K. Kepler, J. Prakash, Electrochim. Acta 52 (2007) 2102–2108.
[19] N. Alexeyeva, A. Sarapuu, K. Tammeveski, F.J. Vidal-Iglesias, J. Solla-Gullón, J.M. Feliu, Electrochim. Acta 56 (2011) 6702–6708.
[20] M. Teo, P.C. Wong, L. Zhu, D. Susac, S.A. Campbell, K.A.R. Mitchell, R.R. Parsons, D. Bizzotto, Appl. Surf. Sci. 253 (2006) 1130–1134.
[21] L. Zhu, D. Susac, A. Lam, M. Teo, P.C. Wong, D. Bizzotto, S.A. Campbell, R.R. Parsons, K.A.R. Mitchell, J. Solid State Chem. 179 (2006) 3942–3948.
[22] D. Susac, A. Sode, L. Zhu, P.C. Wong, M. Teo, D. Bizzotto, K.A.R. Mitchell, R.R. Parsons, S.A. Campbell, J. Phys. Chem. B 110 (2006) 10762–10770.
[23] D. Susac, L. Zhu, M. Teo, A. Sode, K.C. Wong, P.C. Wong, R.R. Parsons, D. Bizzotto, K.A.R. Mitchell, S.A. Campbell, J. Phys. Chem. C 111 (2007) 18715–18723.
[24] L. Zhu, D. Susac, M. Teo, K.C. Wong, P.C. Wong, R.R. Parsons, D. Bizzotto, K.A.R. Mitchell, S.A. Campbell, J. Catal. 258 (2008) 235–242.
[25] E. Vayner, R.A. Sidik, A.B. Anderson, J. Phys. Chem. C 111 (2007) 10508–10513.
[26] Y. Feng, T. He, N. Alonso-Vante, Chem. Mater. 20 (2008) 26–28.
[27] Y. Feng, T. He, N. Alonso-Vante, Electrochim. Acta 54 (2009) 5252–5256.
[28] Y. Feng, T. He, N. Alonso-Vante, Fuel Cells 10 (2010) 77–83.
[29] L. Zhu, M. Teo, P.C. Wong, K.C. Wong, I. Narita, F. Ernst, K.A.R. Mitchell, S.A. Campbell, Appl. Catal. A: Gen. 386 (2010) 157–165.
[30] M. Gao, S. Liu, J. Jiang, C. Cui, W. Yao, S. Yu, J. Mater. Chem. 20 (2010) 9355–9361.
[31] S. Zhang, Y. Shao, H.-G. Liao, J. Liu, I.A. Aksay, G. Yin, Y. Lin, Chem. Mater. 23 (2011) 1079–1081.
[32] K. Lee, L. Zhang, J. Zhang, Electrochem. Commun. 9 (2007) 1704–1708.
[33] M. Bron, P. Bogdanoff, S. Fiechter, I. Dorbandt, M. Hilgendorff, H. Schulenburg, H. Tributsch, J. Electroanal. Chem. 500 (2001) 510–517.
[34] E. Yeager, Electrochim. Acta 29 (1984) 1527–1537.
[35] K. Wiesener, Electrochim. Acta 31 (1986) 1073–1078.
[36] S. Zhang, Y.Y. Shao, G.P. Yin, Y.H. Lin, J. Mater. Chem. 19 (2009) 7995–8001.
[37] K.L. Hsueh, D.T. Chin, S. Srinivasan, J. Electroanal. Chem. 153 (1983) 79–95.
[38] K. Suarez-Alcantara, A. Rodriguez-Castellanos, R. Dante, O. Solorza-Feria, J. Power Sources 157 (2006) 114–120.
[39] S. Zhang, Y.Y. Shao, G.P. Yin, Y.H. Lin, J. Mater. Chem. 20 (2010) 2826–2830.
[40] N. Alonso-Vante, W. Jaegermann, H. Tributshc, W. Honle, K. Yvon, J. Am. Chem. Soc. 109 (1987) 3251–3257.
[41] K. Lee, O. Savadogo, A. Ishihara, S. Mitsushima, N. Kamiya, K. Ota, J. Electrochem. Soc. 153 (2006) A20–A24.